Supplementary Information

Alba shapes the archaeal genome using a delicate balance of bridging and stiffening the DNA

Niels Laurens[1,*], Rosalie P.C. Driessen[2,*], Iddo Heller[1], Daan Vorselen[1], Maarten C. Noom[1], Felix J.H. Hol[1], Malcolm F. White[3], Remus T. Dame[1,2,†], Gijs J.L. Wuite[1,†]

1. Department of Physics and Astronomy, VU University, The Netherlands
2. Leiden Institute of Chemistry and Cell Observatory, Leiden University, The Netherlands
3. Biomedical Sciences Research Complex, University of St. Andrews, UK

*,† *These authors contributed equally to this work*

Corresponding authors: g.j.l.wuite@vu.nl, rtdame@chem.leidenuniv.nl

Supplementary Figures

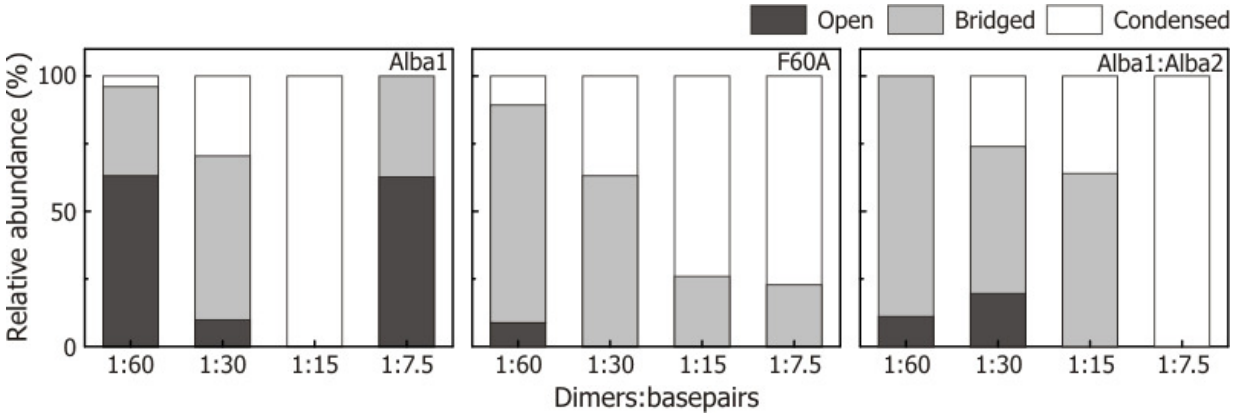

Supplementary figure S1– AFM results

AFM images are analyzed and divided into 3 classes, open (*dark grey*), bridged (*light grey*) and condensed (*white*) (see Materials & Methods in main text for classification method). Shown are the distributions for different concentrations of Alba1 (N = 548 molecules), Alba1 F60A (N = 337 molecules) and the Alba1:Alba2 heterodimers (N = 134 molecules).

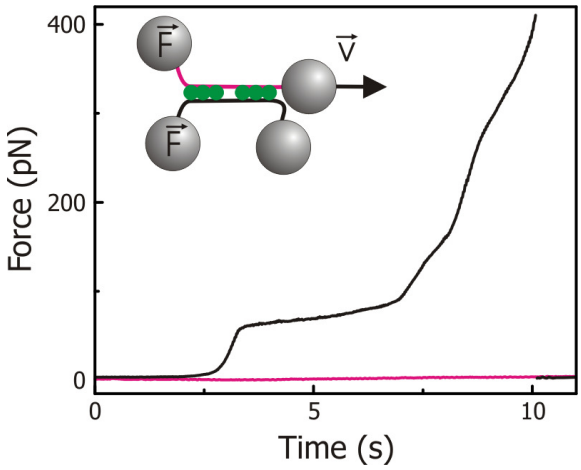

Supplementary figure S2 – Alba bridges are able to withstand high forces
Shown is the force on two DNA molecules bridged by Alba over time, while one of the four beads is moved at a constant speed (*v*), generating a force on the Alba-DNA complex (*black trace*). As can be seen the forces rise to 400 pN before the bead escapes from the optical trap, relaxing the force.

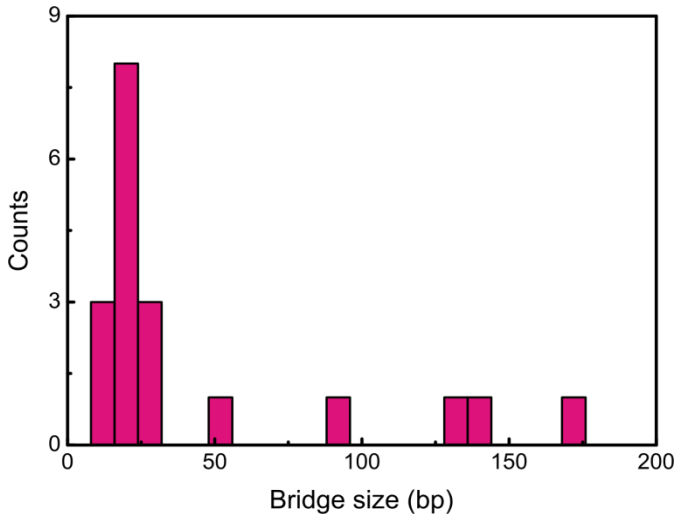

Supplementary figure S3 – Step size distribution of Alba1 F60A bridge ruptures.
Histogram of the amount of base pairs released at a rupture event of a bridge in unzipping experiments with the Alba1 F60A mutant (100 nM, see figure 3b). The distribution shows a peak at ~20 bp (N = 19 events, bin size 8 bp).

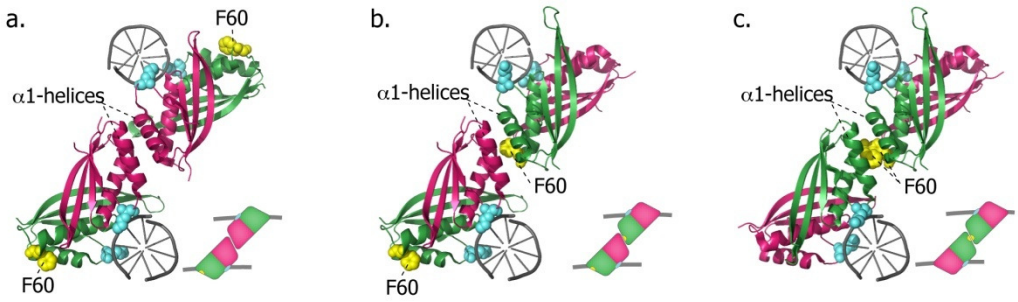

Supplementary **figure S4 – Alba1:Alba2 heterodimer bridging interaction**

Possible configurations of an Alba1:Alba2 heterodimer bridge as shown in figure 4b. **a.** The Alba2 subunits (*magenta*) of the heterodimers can interact by hydrophobic interactions of the α1-helices. **b.** The Alba1 subunit (*green*) can interact with the Alba2 unit (*magenta*) of the opposite dimer. In this configuration the F60 residue on the Alba1 subunit (*yellow*) cannot interact with the Alba2 subunit, due to the absence of an equivalent residue in the Alba2 monomer. **c.** The Alba1 units (*green*) can bridge similar to Alba1 homodimers, using both the hydrophobic interactions of the α1-helices and the additional interaction of the two F60 residues. Cyan shows the K16 residue of the Alba1 unit and the K11 residue of the Alba2 unit, which interact with the minor groove of the DNA. The models are obtained by structural alignment of the Alba1:Alba2 crystal structure (PDB 2BKY[45]) with the co-crystal structure of (Ape10b2)-dsDNA (PDB 2H9U[46]) using PyMol.

Supplementary Table

Protein	Model	c (μM)	L_P (nm)	L_C (μm)	K_0 (pN)	g_0 (pN·nm)	g_1 (nm)	F_c (pN)	N
-	eWLC	0	49 ± 2	15.8 ± 0.4	1600 ± 300				27
Alba1	eWLC	2	260 ± 30	16.2 ± 0.2	2400 ± 600				21
Alba1 F60A	eWLC	5	140 ± 20	16.0 ± 0.1	2200 ± 200				15
Alba1:Alba2	eWLC	1	90 ± 20	16.4 ± 0.1	1800 ± 200				8
Alba1	tWLC	2	240 ± 30	16.3 ± 0.1	2100 ± 300	560 ± 100	19 ± 6	31 ± 7	10

Supplementary **table S1 – eWLC & tWLC fitting parameters**

Extensible worm-like chain and twistable worm-like chain fitting parameters as obtained from fitting FD curves to equation (1). Shown for bare DNA (-) and highest measured protein concentrations of Alba1 (2 μM), Alba1 F60A (5 μM), and the Alba1:Alba2 heterodimers (1 μM). Values are averages of N individual DNA molecules and indicated error is given as the standard error of the mean.

Supplementary References

45 Jelinska, C. *et al.* Obligate heterodimerization of the archaeal Alba2 protein with Alba1 provides a mechanism for control of DNA packaging. *Structure* **13**, 963-971, (2005).

46 Tanaka, T., Padavattan, S. & Kumarevel, T. Crystal Structure of Archaeal Chromatin Protein Alba2-Double-stranded DNA Complex from Aeropyrum pernix K1. *J Biol Chem* **287**, 10394-10402, (2012).